CASE FILE COPY

NACA

RESEARCH MEMORANDUM

HIGH-SPEED WIND-TUNNEL TESTS OF A $\frac{1}{16}$ -SCALE MODEL

OF THE D-558 RESEARCH AIRPLANE

LONGITUDINAL STABILITY AND CONTROL OF THE D-558-1

Ву

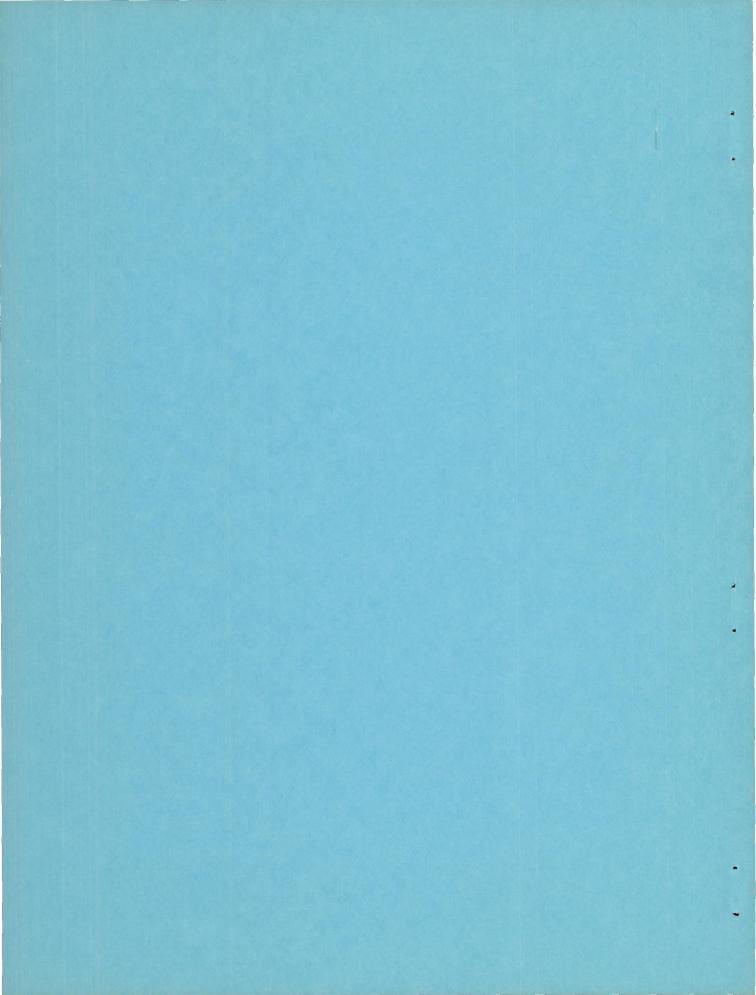
John B. Wright

Langley Memorial Aeronautical Laboratory Langley Field, Va.

NATIONAL ADVISORY COMMITTEE FOR AERONAUTICS

WASHINGTON

July 8, 1948
Declassified August 18, 1954



NATIONAL ADVISORY COMMITTEE FOR AERONAUTICS

RESEARCH MEMORANDUM

HIGH-SPEED WIND-TUNNEL TESTS OF A $\frac{1}{16}$ -SCALE MODEL OF THE D-558 RESEARCH AIRPLANE

LONGITUDINAL STABILITY AND CONTROL OF THE D-558-1

By John B. Wright

SUMMARY

This paper contains the results of pitching-moment and lift measurements with a $\frac{1}{16}$ -scale model of the D-558-1 airplane with no nose-inlet flow at several tail and elevator settings. Tests were conducted through a Mach number range up to 0.96 in the Langley 8-foot high-speed tunnel. In order to facilitate forwarding of this information, only a limited analysis is presented.

Tests with various control deflections show serious changes in stability above a Mach number of 0.86 with a tendency for the airplane to become unstable around a Mach number of 0.9 at varying low lift coefficients, dependent on the control setting. Downwash changes do not appear to be responsible for the adverse stability.

Control effectiveness by variable stabilizer incidence is indicated to be feasible throughout the Mach number range tested. For the elevator—angle range investigated, it is indicated that elevator control becomes unsatisfactory because a reversal in effectiveness occurs for small deflections at a Mach number of approximately 0.85. At higher Mach numbers, the trend obtained indicates an increasing range of deflections where reversal occurs. Increases in downwash and decreases in stabilizer and control effectiveness with increases in Mach number are indicated to be the cause for large changes in control settings for trim above an approximate Mach number of 0.9.

INTRODUCTION

The D-558-1 is a research airplane designed to investigate aero-dynamic phenomena in the transonic speed range. It is designed to fly at a level-flight Mach number of 0.85 and is powered by a turbojet unit. It has an unswept wing of aspect ratio 4.17 in a low position on the fuselage.

Wind-tunnel tests of a $\frac{1}{16}$ -scale model were conducted to high subsonic Mach numbers in the Langley 8-foot high-speed tunnel in order to provide preflight information for the pilot to insure against any catastrophic events due to compressibility effects during flight.

This paper presents lift and pitching-moment results obtained from an internal-balance system with a $\frac{1}{16}$ -scale model of the D-558-1 with several stabilizer and elevator settings without nose-inlet flow. Reference 1 contains results for the model with one tail setting and with the tail off. In order to expedite this information to the NACA flight-test group at Muroc, Calif., to the manufacturer, Douglas Aircraft Company, and to the Navy Bureau of Aeronautics, this report contains only the results available at the present time with a limited analysis.

APPARATUS AND TECHNIQUE

The D-558 investigation was conducted in the Langley 8-foot high-speed tunnel, which is a single-return closed-throat type. The maximum corrected test Mach number was approximately 0.96 for this investigation. The Reynolds number varied from about 1.0 \times 106 to 1.6 \times 106 based on a mean aerodynamic chord of 4.656 inches.

Model.— An all-metal $\frac{1}{16}$ -scale model of the D-558-l airplane was constructed by the NACA. The general layout is shown by the three-view drawing in figure 1. The geometry and dimensions of the wing and tail are given in table I. Since no inlet flow was simulated, the nose inlet was faired forward to form a solid nose and to maintain smooth flow conditions. The fuselage was hollow to allow for the internal balance.

Model support and balance.— The sting—strut support system used in these tests is shown in figure 2. The sting, containing the balance within the fuselage, was attached to the fuselage inside and well forward. The sting diameter is smaller than the inside diameter of the fuselage so that all aerodynamic forces are transmitted through the balance. The sting enlarges smoothly aft of the model to the angle—of—attack coupling, thence to the support strut. In an attempt to avoid choking the tunnel at the strut location at a low test—section Mach number, a liner to constrict the flow was installed in the throat of the tunnel and designed to obtain the highest possible test Mach numbers at the model location.

The balance consisted of strain-gage elements located on the sting and on component parts of the sting so as to measure pitching moment, normal force, and axial force. A transferral of forces to the airplane

center of gravity was required because the pitching moment was found at the center of the pitching-moment-gage location which is a small distance from the center of gravity. Further, the normal force had to be reoriented to the lift direction by simple trigonometry. Thus, the data presented are referred to the wind axes.

Two types of tare runs were made for several configurations to evaluate the interference of the sting on the model. The tare-measuring arrangement is shown in figures 2 and 3. The tare setup incorporated auxiliary tare arms which had 6-percent-thick airfoils swept back 30° in forward portions to minimize high-speed interference effects. The arms were attached in the model to an internal balance similar to that used with the sting for the normal runs. In this tare arrangement it is assumed that there is no interference of the arms on the sting.

Corrections. All data were referred to a center-of-gravity location of 25 percent mean aerodynamic chord shown in figure 1. The data were corrected for angle-of-attack changes due to bending of the sting and strain-gage balance beams by determining the angle at each test point and interpolating to obtain constant angle of attack. The angle of attack used herein is that of the fuselage center line. The effect of temperature on the strain gages was determined in static-load and temperature tests. The temperature of the gages was measured during each run and the corresponding small corrections found in static tests were applied.

The data have all been corrected for the interference of the sting by measuring this effect by the two types of tare runs shown in figure 3. It was found that the sting produced an interference on pitching-moment coefficient which averaged 0.020 over the Mach number and angle-of-attack ranges. The interference of the sting on lift coefficient was negligible.

The data are presented to a corrected Mach number of about 0.96. Choking due to wake effects occurred at the strut. However, there was less than 0.01 Mach number difference in the theoretical choking Mach number at the model location and that attained in these tests. The data are unaffected by choke phenomena because the strut is well aft of the model and tunnel calibration measurements indicated no irregularities in the model test section.

While Reynolds number effects may modify the absolute values of data with respect to the full-scale airplane, it is believed that general effects shown are chiefly the result of compressibility phenomena. Reynolds numbers here appear to be larger than the critical values shown in other investigations.

Corrections for wind-tunnel effects have been applied to these data in the manner indicated in references 1 and 2.

RESULTS AND DISCUSSION

Stability

Figure 4 presents the variation of pitching-moment and lift coefficient with Mach number for constant angles of attack for the model with tail incidence, $i_{\rm t}=0.3^{\circ},\,2.2^{\circ},\,4.0^{\circ},\,$ and 6.2° with elevator angle, $\delta_{\rm e}=0^{\circ}$. In figure 5 the data from figure 4 and reference 1 (model less tail) have been used to show the variation of pitching-moment coefficient with lift coefficient for various Mach numbers. Figure 6 presents the variation of lift and pitching-moment coefficients with Mach number for constant angles of attack for the model with $\delta_{\rm e}=-4^{\circ},$ $-2^{\circ},\,2^{\circ},\,4^{\circ},\,$ and 6° with $i_{\rm t}=2.2^{\circ}.$ The data in figures 6 and 4(b) $(\delta_{\rm e}=0^{\circ})$ are cross plotted in figure 7 to show the variation of pitching-moment coefficient with lift coefficient for various Mach numbers. From the results shown in the preceding figures, it is evident that the unstable tendency, first shown in reference 1, around a Mach number of 0.9 and at low lift coefficients occurs at all tail incidences or elevator angles measured.

Figure 8 shows the lift coefficients required for level flight at two altitudes with a wing loading of 66.7 pounds per square foot corresponding to an airplane weight of 10,000 pounds. The slope $\partial C_m/\partial C_T$ the stability curves of figure 5 is shown in figure 9 for the four tail incidences at two altitude level-flight (untrimmed) conditions (fig. 8). Figure 10 shows the static longitudinal stability parameter $\partial C_m/\partial C_L$ obtained at trim conditions by interpolation of the data in figure 9 for the required trim tail incidences. Because of small shifts in the lift coefficient where the instability occurs at different tail incidences (figs. 5 and 9), it is indicated that increased stabilizer settings will tend to reduce the unfavorable stability changes in level flight even at sea level. Because of this fact, the stability indicated at trim conditions (fig. 10) appears to be satisfactory. Furthermore, since the unstable tendency occurs over a small lift-coefficient range, the behavior of the airplane may be merely uncomfortable rather than unsafe if these regions are entered. Further analysis concerning the dynamic response to these imposed aerodynamic loadings must be made to determine this characteristic.

It will be shown herein that downwash effects are probably not responsible for the tendency towards the instability just shown. It remains then that the wing-fuselage characteristics are chiefly responsible for the phenomenon. It is believed, as tests of airfoils at supercritical speeds have shown (reference 3), that as the Mach number is increased there is a forward movement of the center of pressure of the wing following the usual rearward supercritical movement. This shift in the center of

pressure probably causes the instability noted. A similar effect was noted with a wing of symmetrical sections (reference 4) mounted on the D-558-1 fuselage.

Control

In figure 7 is shown the loss of elevator effectiveness as the Mach number approaches approximately 0.90. Further, reversal of elevator control within the range tested appears to be established at the highest test Mach number. Stabilizer effectiveness, however, (fig. 5) is not seriously reduced through the highest test Mach number.

The preceding phenomena are shown in more detail in the following figures. Figure 11 shows the lift coefficient at $C_m=0$ for various tail incidences and elevator angles as a function of Mach number. Two trim points are indicated at a Mach number of 0.905 for the $i_t=4^{\circ}$ case. The elevator-control reversal shown occurs at lift coefficients greater than those required in level flight at these high Mach numbers. It will be necessary to obtain greater deflections of the elevator in this investigation to define completely the behavior of the elevator in level flight. Figure 12 shows the variation of lift coefficient at $C_m=0$ with tail incidence and elevator angle for various Mach numbers. It appears from the trends indicated in this figure that the reversal occurs for a range of small elevator deflections and that the range increases with Mach number.

Figure 13 presents the Mach number variation of tail incidence, with the elevator angle at 0°, required for trim and the elevator angle, with the tail incidence at 2.2°, required for trim obtained from figure 12 at lift coefficients required for level flight at two altitudes. Large changes in these tail settings are required above a Mach number of 0.85. The two trim points at a Mach number of 0.905 cause two possible required tail incidences at this Mach number, but it is believed that the larger incidence will be utilized in conventional flight. Extreme changes in elevator angle precede the reversal effects which, at 35,000 feet, become apparent near a Mach number of 0.93.

The variation of pitching-moment coefficient with control deflections for several Mach numbers is shown in figure 14. The pitching-moment coefficients at each Mach number were chosen at the lift coefficients corresponding to the two level-flight altitude conditions. The slopes $\partial C_m/\partial i_t$ and $\partial C_m/\partial \delta_e$ representing stabilizer and elevator effectiveness, respectively, at the trim condition, were obtained from figure 14 at $C_m=0$ and are shown in figure 15 as a function of Mach number. The principal characteristic indicated is the serious reduction and reversal of elevator effectiveness beyond a Mach number of 0.93 for this tail incidence.

It is believed that earlier and more adverse elevator characteristics would be felt than indicated in figure 15(b) if the tail incidence were set for a higher speed trim setting. Small elevator deflections would then be ineffective or cause reversed effects at high Mach numbers (fig. 14(b)). Conventional effectiveness could be attained only with increasing deflections at increasing Mach numbers. Although a small loss in stabilizer effectiveness above a Mach number of 0.85 is indicated, it appears that this method of control will be advisable in this speed range because of the loss in elevator effectiveness. At a Mach number of 0.95, the stabilizer effectiveness has almost reattained its low-speed value.

Downwash

The effective downwash at the tail could be determined by the addition of the tail incidence to the angle of attack where the tail lift is zero because the horizontal tail is symmetrical. Zero tail lift was determined by finding the points where the pitching moment of the complete model and model without horizontal tail is the same. In this determination, it has been assumed that the drag and pitching moment of the tail have no effect on pitching moment. From figure 5, the lift coefficients where the pitching-moment coefficients of the complete model and the model without horizontal tail are equal $(\Delta C_m = 0)$ were obtained and are shown as a function of Mach number in figure 16 for the four tail incidences. The angles of attack corresponding to these lift coefficients were determined and are shown in figure 17. The effective downwash has been determined by addition of the tail incidence it to the angle of attack where $\Delta C_{\rm m}$ = 0 (fig. 17) for each incidence tested. This effective downwash is shown in figure 18 as a function of Mach number for the four tail incidences.

From figures 16 and 18, the variation of effective downwash with lift coefficient was obtained as shown in figure 19. The rate of change of downwash with lift coefficient $\partial \epsilon/\partial c_{\mathrm{L}}$ at level-flight lift coefficients at two altitudes is shown in figure 20. These downwash curves indicate that the unstable tendency noted at low lift coefficients at an approximate Mach number of 0.9 is probably not caused by adverse downwash characteristics. An increase in the rate of change of downwash with lift coefficient is destabilizing, but, as indicated in figure 20, there is no increase in $d \in /dC_{\mathrm{L}}$ in this Mach number and lift-coefficient range. On the contrary, there are large decreases (stabilizing) in $d\varepsilon/dC_{\rm L}$ shown occurring in the same ranges that are evidently counteracted by large tail-off instability. It should be noted that the slopes were obtained at level-flight lift coefficients as was the stability parameter $\partial C_{\rm m}/\partial C_{\rm L}$ in figure 10, and that for this condition little tendency towards instability was found. Because of the nature of this downwash determination and the fact that the unstable region varies with tail setting, it is possible that some downwash characteristics may be obscured.

Figure 21 shows the variation of $\partial \epsilon/\partial \alpha$ with Mach number. The effective downwash for level-flight conditions at two altitudes is shown in figure 22 as a function of Mach number. A point of notation is the increase in downwash for level-flight lift coefficients, or even constant lift coefficients, above 0.875 Mach number. The increase in downwash combines with decreased stabilizer and elevator effectiveness to make necessary large increases in tail settings.

CONCLUDING REMARKS

From tests of a $\frac{1}{16}$ -scale model of the D-558-1 airplane with no nose-inlet flow and with several tail and elevator settings, the following remarks have been indicated:

- 1. The airplane can experience large changes in stability beyond a Mach number of 0.86. An unstable tendency at approximately a Mach number of 0.9 occurs, the severity and location of which with respect to lift coefficient are dependent on tail setting.
- 2. Effective downwash characteristics do not appear to contribute to the instability noted. It remains then that large center-of-pressure changes, as evidenced by the horizontal tail-off tests, with possible changes in the lift-curve slope of the tail probably account for the large stability changes.
- 3. Stabilizer effectiveness decreases slightly and incidence required increases beyond a Mach number of 0.85, but it is indicated that control by this means is possible and advisable through a Mach number of 0.96.
- 4. Elevator control, however, is shown to be unsatisfactory beyond Mach numbers of approximately 0.85, depending on tail-incidence setting because of a reversal for small elevator deflections. The range of deflections wherein reversed elevator control is indicated increases with increases in Mach number.

- 5. Increases of downwash and decreases in control effectiveness with increases in Mach number are indicated to be the cause for the large increases in tail settings required for trim in the Mach number = 0.9 region.
- Langley Memorial Aeronautical Laboratory
 National Advisory Committee for Aeronautics
 Langley Field, Va.

REFERENCES

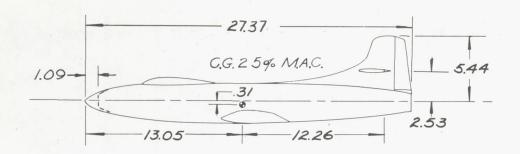
- 1. Wright, John B.: High-Speed Wind-Tunnel Tests of a 1/16-Scale Model of the D-558 Research Airplane. Basic Longitudinal Stability of the D-558-1. NACA RM No. L7K24, 1947.
- 2. Wright, John B., and Loving, Donald L.: High-Speed Wind-Tunnel Tests of a 1/16-Scale Model of the D-558 Research Airplane. Lift and Drag Characteristics of the D-558-1 and Various Wing and Tail Configurations. NACA RM No. L6J09, 1946.
- 3. Bielat, Ralph P.: An Investigation at High Speeds of a Horizontal-Tail Model in the Langley 8-Foot High-Speed Tunnel. NACA RM No. L6LlOb, 1947.
- 4. Wright, John B.: High-Speed Wind-Tunnel Tests of a $\frac{1}{16}$ -Scale Model of the D-558 Research Airplane. D-558-1 Speed Reduction Brake and Symmetrical-Profile Wing Characteristics. NACA RM No. L8B06, 1948.

TABLE I

WING AND TAIL DIMENSIONS OF $\frac{1}{16}$ -SCALE D-558-1 MODEL

Wing section
Wing aspect ratio 4.17
Wing taper ratio
Wing span, in
Wing area, sq ft
Wing mean aerodynamic chord, in 4.656
Wing incidence angle, deg
Wing dihedral, deg
Wing sweep angle (50 percent chord), deg
Wing root chord, in
Wing tip chord, in
Longitudinal location of 25-percent-mean-aerodynamic-chord point from nose-inlet station, in. (also center-of-gravity location)
Tail section
Tail aspect ratio
Tail taper ratio
Tail span, in
Tail area, sq ft
Tail dihedral, deg
Tail sweep angle (75 percent chord), deg 0
Elevator area, percent of tail area

NACA



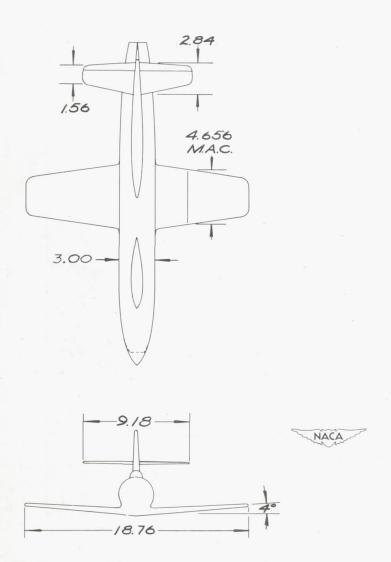


Figure | - Drawing of 1/16-scale D-558-1 model as tested in the Langley 8-foothigh-speed tunnel. All dimensions in inches.

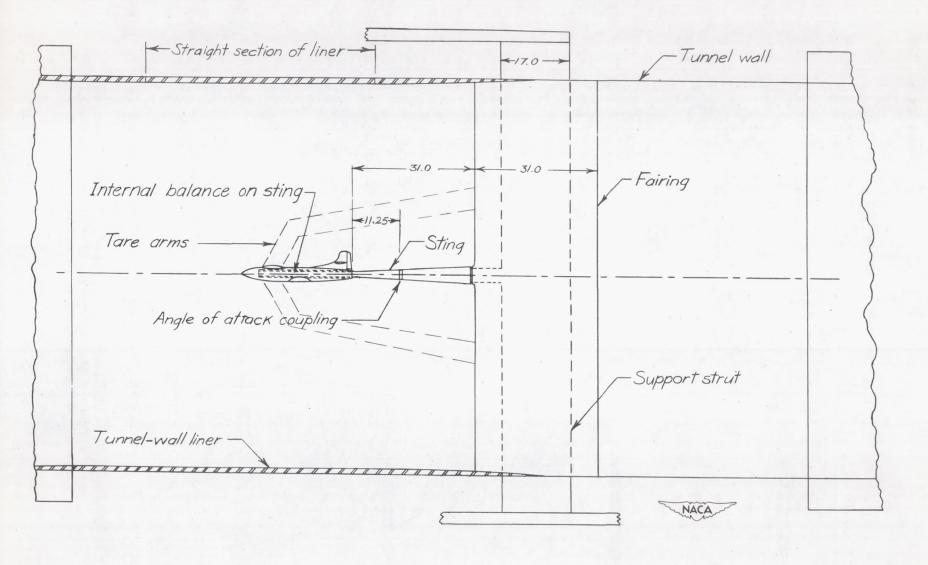
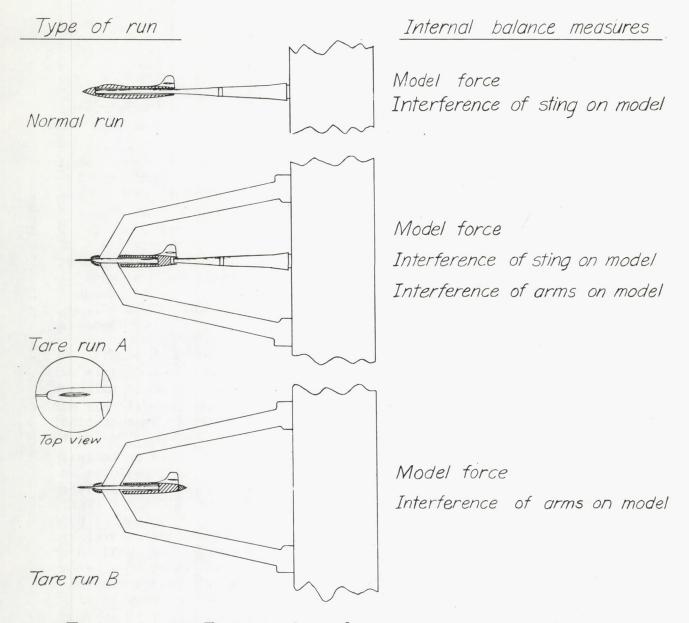


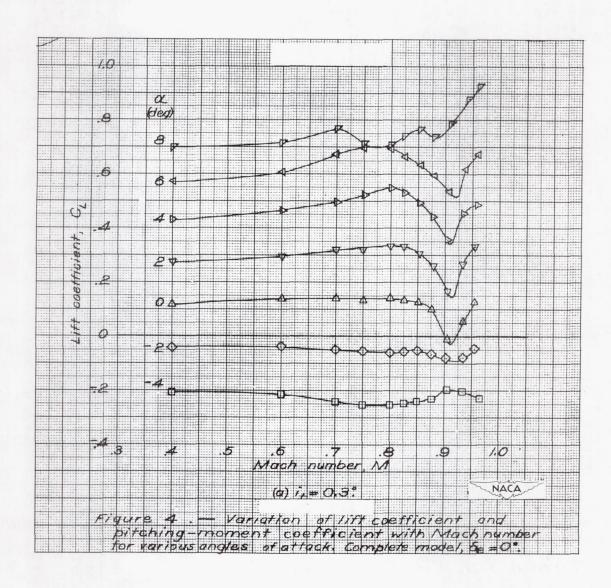
Figure 2 .- Model on sting support in the Langley 8-foot high-speed tunnel All dimensions in inches.

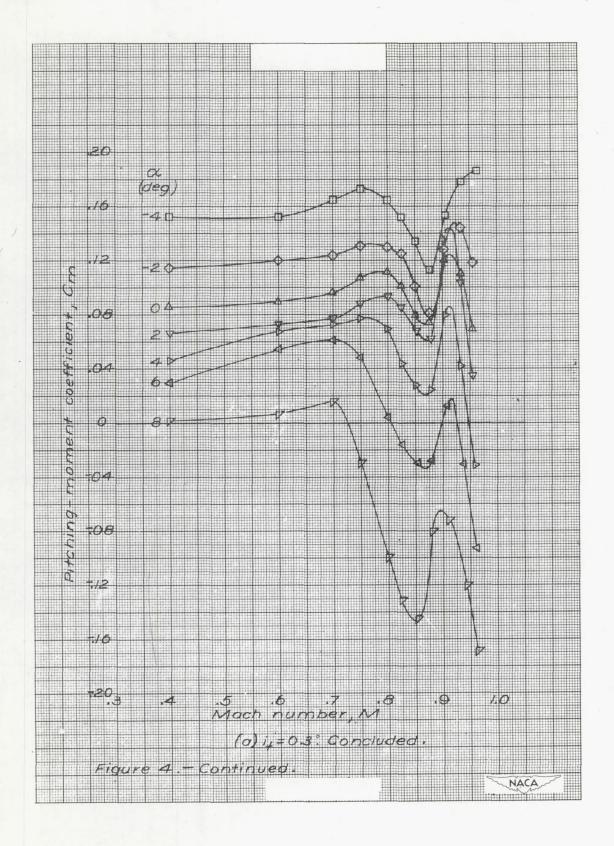


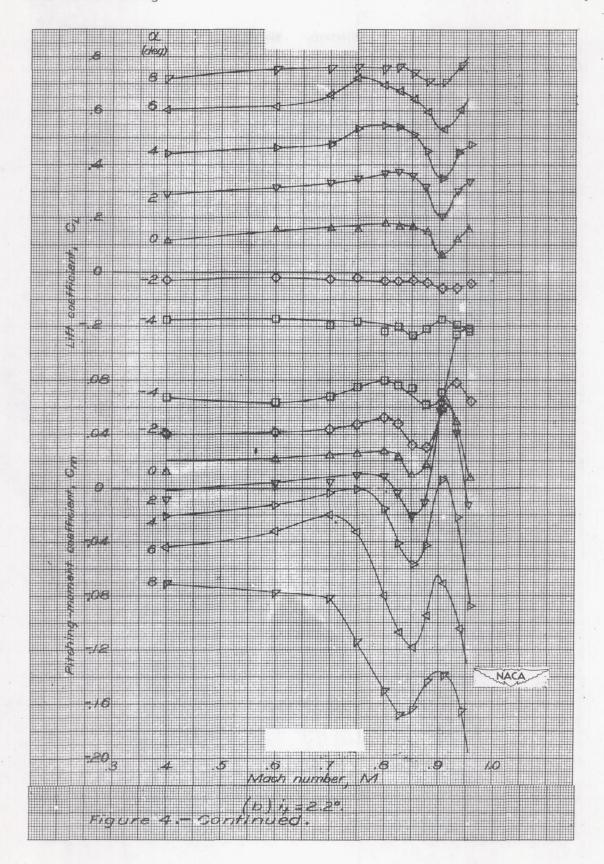
Tare run A - Tare run B = Interference of sting on model

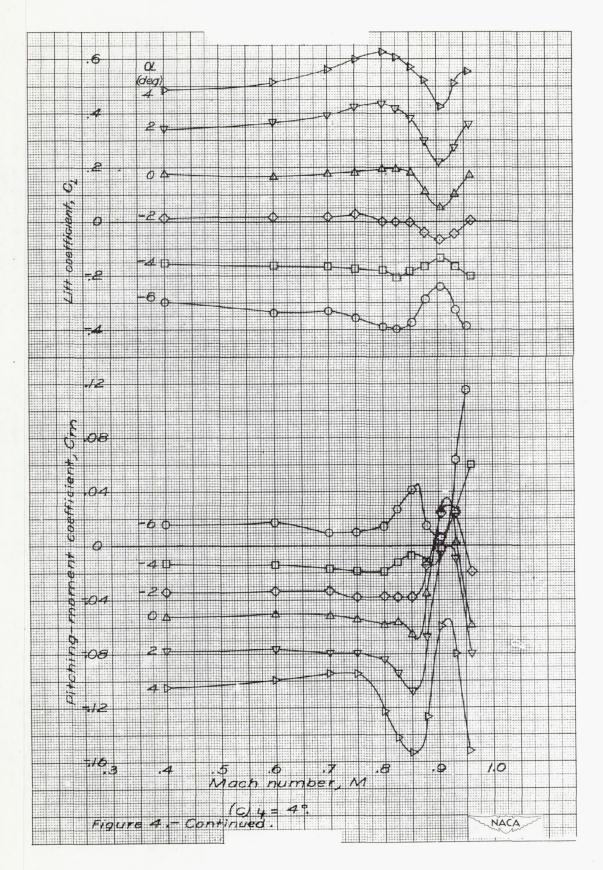
Normal run - (A-B) = Model force

Figure 3.-Model setups and tare evaluation technique.

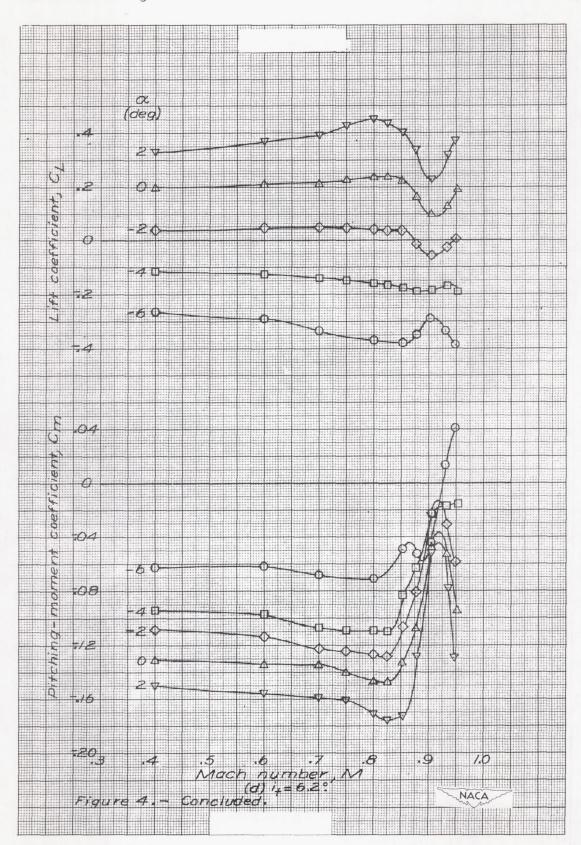








C



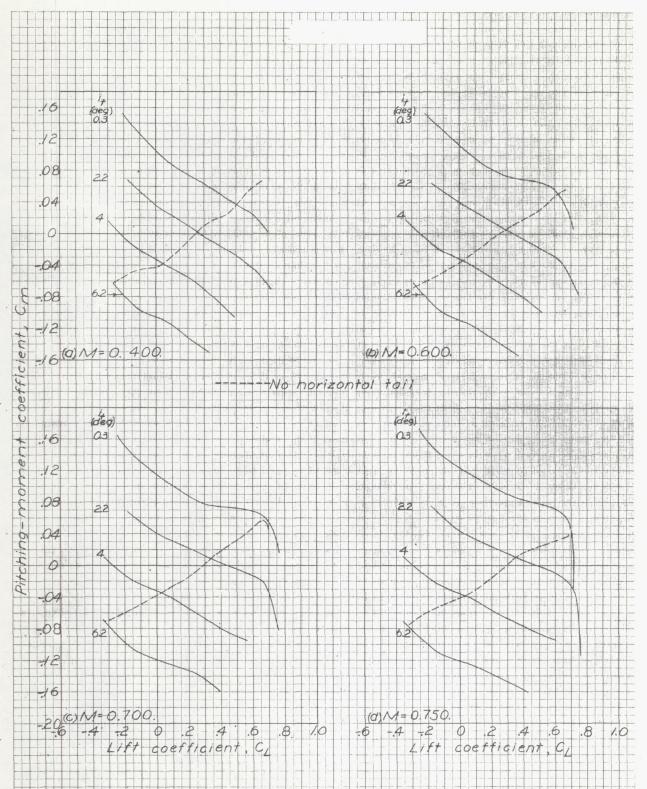
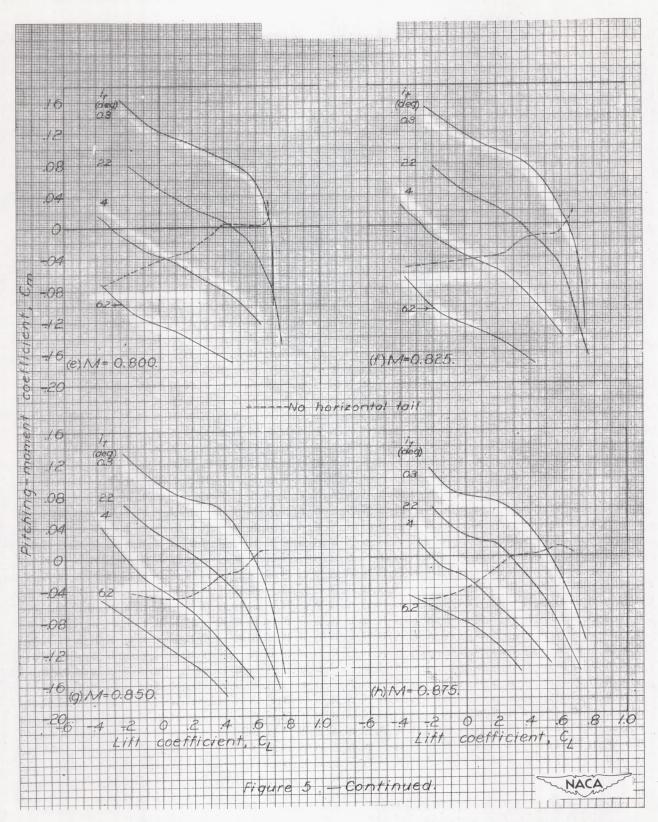
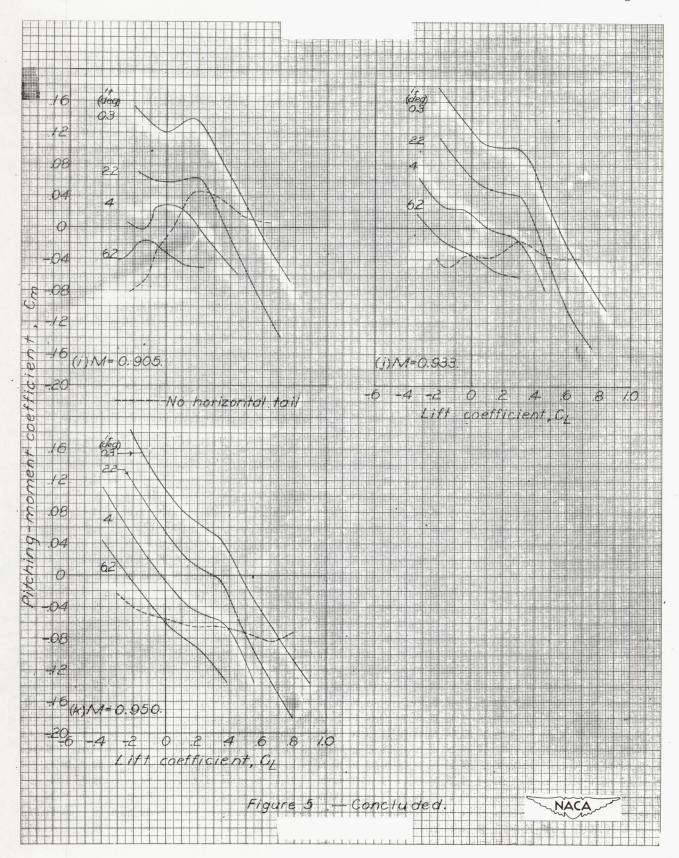
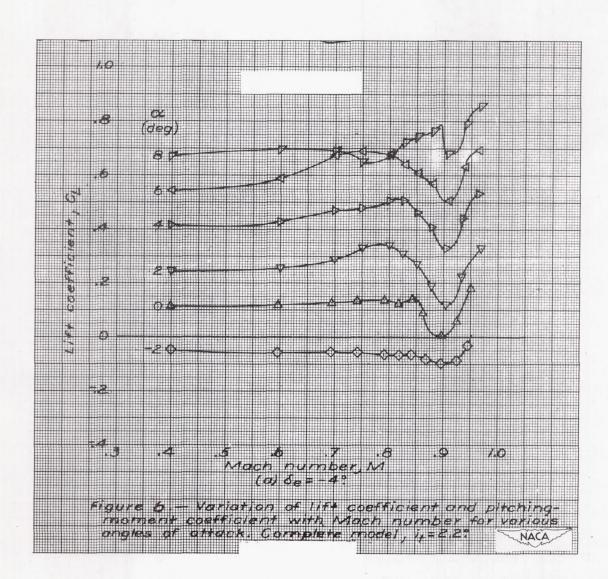
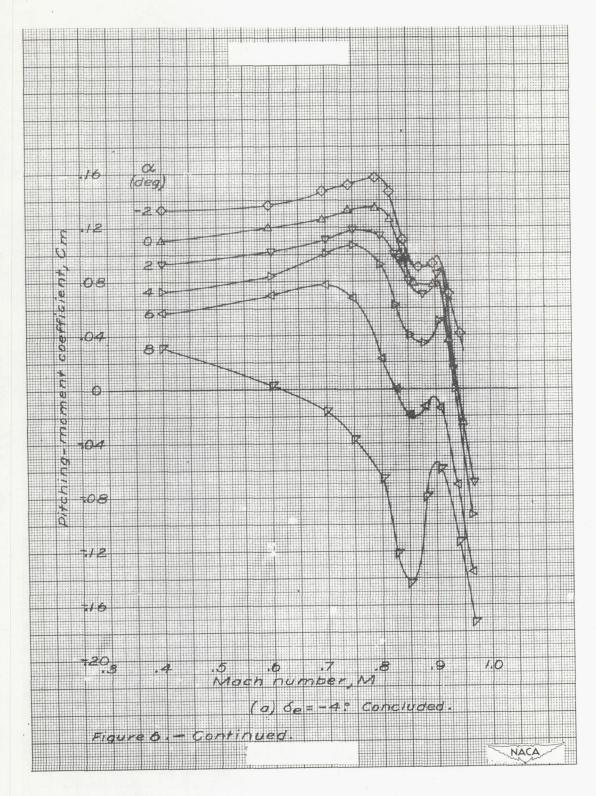


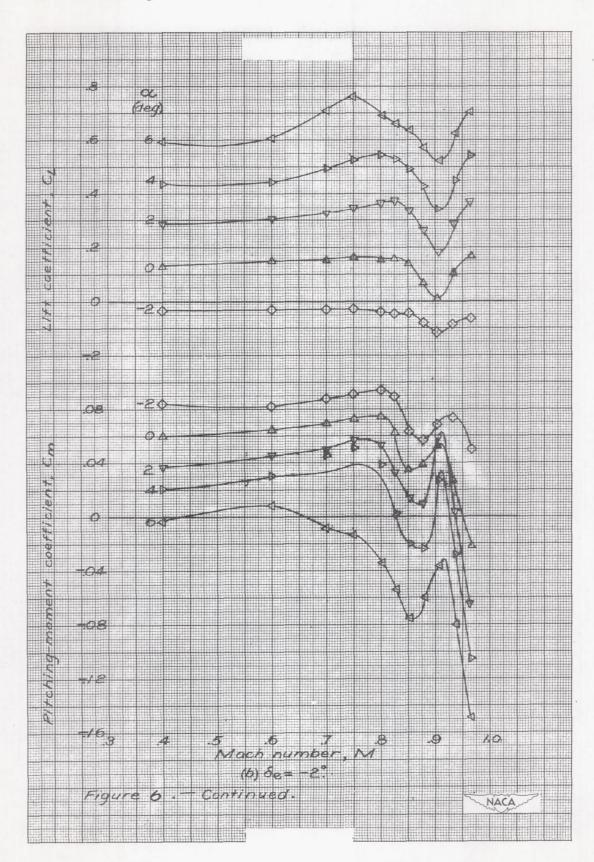
Figure 5 - Variation of pitching-moment coefficient with lift coefficient for various Mach numbers. Complete model, 6e=0, and model less harizontal tail.

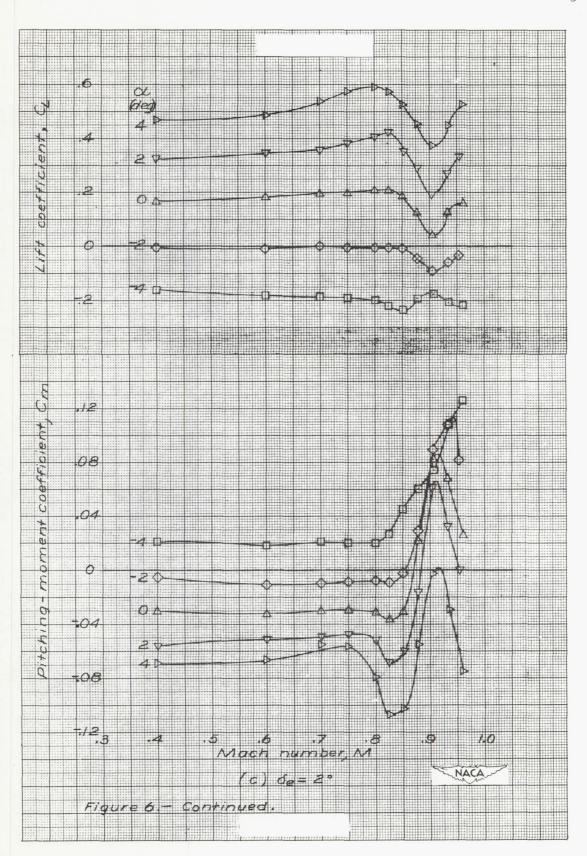












C

